Annales Geophysicae (2004) 22: 3363–3374
SRef-ID: 1432-0576/ag/2004-22-3363

Annales Geophysicae

Cup anemometer response to the wind turbulence – measurement of the horizontal wind variance

S. Yahaya and J. P. Frangi

Laboratoire Environnement & Développement, CP 7071, Université Paris 7 – Denis Diderot, 2 Place Jussieu, 75251 Paris Cedex 05, France

Received: 19 January 2004 – Revised: 8 July 2004 – Accepted: 20 July 2004 – Published: 3 November 2004

Abstract. This paper presents some dynamic characteristics of an opto-electronic cup anemometer model in relation to its response to the wind turbulence. It is based on experimental data of the natural wind turbulence measured both by an ultrasonic anemometer and two samples of the mentioned cup anemometer. The distance constants of the latter devices measured in a wind tunnel are in good agreement with those determined by the spectral analysis method proposed in this study. In addition, the study shows that the linear compensation of the cup anemometer response, beyond the cutoff frequency, is limited to a given frequency, characteristic of the device. Beyond this frequency, the compensation effectiveness relies mainly on the wind characteristics, particularly the direction variability and the horizontal turbulence intensity. Finally, this study demonstrates the potential of fast cup anemometers to measure some turbulence parameters (like wind variance) with errors of the magnitude as those deriving from the mean speed measurements. This result proves that fast cup anemometers can be used to assess some turbulence parameters, especially for long-term measurements in severe climate conditions (icing, snowing or sandy storm weathers).

Key words. Meteorology and atmospheric dynamics (turbulence; instruments and techniques; general)

1 Introduction

Due to specific characteristics (robustness, reliability and relative low cost) and despite well-known drawbacks (overestimation of mean wind speed, inertial effects at higher frequencies), the response of cup anemometers to the wind turbulence is widely studied to better understand the overestimation mechanism (Kristensen, 1998), to define accurate estimators of turbulence parameters (Weber, 1998), and to improve data analysis methodologies (Hristov et al., 2000). Although the sonic anemometer is considered as the appropriate tool to study wind turbulence, it can, however, fail in some circumstances, for instance, in the case of long period measurements under rainy, snowing, icing or sandy storm climates (Makkonen et al., 2001). In those conditions, other apparatus such as fast cup anemometers might be considered (Yahaya et al., 2003).

Two approaches are currently explored to improve cup anemometers performances. The first one consists in lowering the constant distance of the apparatus, thus improving its time constant (Frenzen, 1988). The second one is to define a compensation method, taking into account the dynamic characteristics of the device (Hristov et al., 2000). A third way, more trivial, is to adopt variable calibration constants fitting to wind speed intervals.

Experimenters often have to face the problem of the choice of an appropriate sampling rate since little information is usually provided by manufacturers. Some people commonly choose a sampling rate of few Hz (Frangi and Richard, 2000), while others sample at 10 Hz or more (Hristov et al., 2000) to improve the data accuracy. In that case, the knowledge of the spectral characteristics of the cup anemometer response could be very helpful, avoiding the use of unnecessary high sampling rates.

The distance constant of cup anemometers is usually determined in wind tunnels according to well-established protocols[1]. But given that it conditions the apparatus behavior in turbulent environment, it is possible to determine its value with a spectral study of the anemometer response, as reported by Kristensen and Hansen (2002). Unlike the wind tunnel methodology which provides both the accelerating and the decelerating distance constants, the one from the spectral study determines a practical value of the two constants. The method proposed by these authors is based on the determination of an experimental transfer function between the cup anemometer and an ultrasonic anemometer. However,

Correspondence to: J. P. Frangi
(frangi@moka.ccr.jussieu.fr)

[1] e.g. the American Standard "D5096-02 Standard Test Method for Determining the Performance of a Cup Anemometer"

it requires an adjustment taking into account a possible calibration discrepancy between the two anemometers and it presumes that the two devices are responding to the same excitation signal (fluctuating wind). Even if the data measured by the anemometers are generally highly correlated, they are nonetheless not totally similar.

Furthering the previous idea, this paper proposes a comparison between the power spectra of the ultrasonic and the cup anemometers. Thus, the right distance constant value is the one that minimises the difference between the two spectra. It is clear that the accuracy of both methods depends on the considered spectral range. It then appears important to assess the upper limit of the meaningful spectrum. In addition, this limit constitutes the highest useful sampling rate frequency for experimental measurements.

In the first part of this paper, equations related to the computation of the cup anemometer transfer function and to the determination of the distance constant in the wind tunnel are stated. The second part presents the experimental instrumentation and protocol. The results, commented in the third part, focus on the calculation method of the distance constant, the upper frequency limit of the anemometer meaningful spectrum and the measurement of wind speed variance.

2 Theoretical background

2.1 Cup anemometer response to wind fluctuations

Within a certain wind bin and in a laminar flow, the wind speed, u_a, measured by the cup anemometer is related to the angular velocity of the device by:

$$u_a(t) = ls(t) + U_0\,, \tag{1}$$

with l the calibration constant, U_0 the threshold speed, and t the time.

When only the first order fluctuations parameters are accounted for, the dynamic response of the cup anemometer is described by Kristensen (1998):

$$\tau \frac{ds'(t)}{dt} + s'(t) = \frac{1}{l}\left(u'(t) + \mu w'(t)\right)\,, \tag{2}$$

where $s'(t)$ is the fluctuation of the cup anemometer angular velocity, $u'(t)$ and $w'(t)$ are the fluctuations of the longitudinal and vertical wind speed, respectively, τ is the cup anemometer time constant and μ is a constant. From Eq. (2), we derive the spectral transfer function (see Appendix A), $F_T(\omega)$:

$$F_T(\omega) = \frac{l^2 P_s(\omega)}{P_u(\omega) + \mu^2 P_w(\omega) + \mu P_{uw}(\omega)} \approx \frac{1}{1+\omega^2\tau^2}\,, \tag{3}$$

where ω is the pulsation and P_a, P_u and P_w are the spectral intensities of the cup anemometer velocity, the longitudinal and vertical wind speeds, respectively. P_{uw} is the cross-spectral intensity of the longitudinal and the vertical speeds. According to MacCready and Jex (1964), the multiplication of τ by the mean wind speed U is always constant and equal to the cup anemometer distance constant, i.e.:

$$L = U \cdot \tau\,. \tag{4}$$

Thus, Eq. (3) becomes:

$$F_T(\omega) = \frac{1}{1+\frac{\omega^2 L^2}{U^2}} \tag{5}$$

with L the distance constant and U the mean wind speed. The signal amplitude attenuation is then given by:

$$\alpha = \frac{1}{\sqrt{1+\frac{\omega^2 L^2}{U^2}}}\,. \tag{6}$$

2.2 Cup anemometer response to mean wind variation – determination of the constant distance in wind tunnel

For a laminar flow, for example in wind tunnels, Eq. (2) can, before equilibrium between $s(t)$ and $u(t)$, be written as follows:

$$\tau \frac{ds(t)}{dt} + s(t) = \frac{1}{l}\left(U - U_0\right)\,, \tag{7}$$

where U is the constant wind speed in the wind tunnel.

Let us consider a situation where the wind-tunnel speed is changed instantly at time t_1 from U_1 to U_2. Then let us replace the time constant by its expression in Eq. (4). Thus, Eq. (7) becomes (see Appendix B):

$$\frac{ds(t)}{dt} = \frac{l(t)+U_0}{lL}\left(U_2 - ls(t) - U_0\right)\,. \tag{8}$$

If S_1 and S_2 are the angular velocities corresponding to U_1 and U_2, and if we integrate this equation between U_1 and a given speed U, we obtain (see Appendix B):

$$\ln\left(\frac{lS+U_0}{U_2-U_0-lS}\right) - \ln\left(\frac{lS_1+U_0}{U_2-U_0-lS_1}\right) = \frac{U_2}{L}\left(t-t_1\right)\,, \tag{9}$$

which can be rewritten as:

$$\frac{lS_2+U_0}{lS+U_0} - 1 = \frac{U_2-U_0-lS_1}{lS_1+U_0}\exp\left(\frac{U_2 t_1}{L}\right)\exp\left(-\frac{U_2}{L}t\right) \tag{10a}$$

or

$$f(t) = \frac{lS_2+U_0}{lS+U_0} - 1 = B\,e^{-At} \tag{10b}$$

with $A = \frac{U_2}{L}$ and $B = \frac{U_2-U_0-lS_1}{lS_1+U_0}\exp\left(\frac{U_2 t_1}{L}\right)$.

Let consider the case where the cup anemometer is put in a wind tunnel with a constant speed U_2. A card is introduced upstream from the anemometer until it stops. Then the card is removed to let the flow pass through the anemometer. Thus, we obtain the curve in Fig. 1. From the ascending phase of Fig. 1 and after removing the threshold speed part, we can determine the constant distance through the following process (cf. Yahaya, 2004):

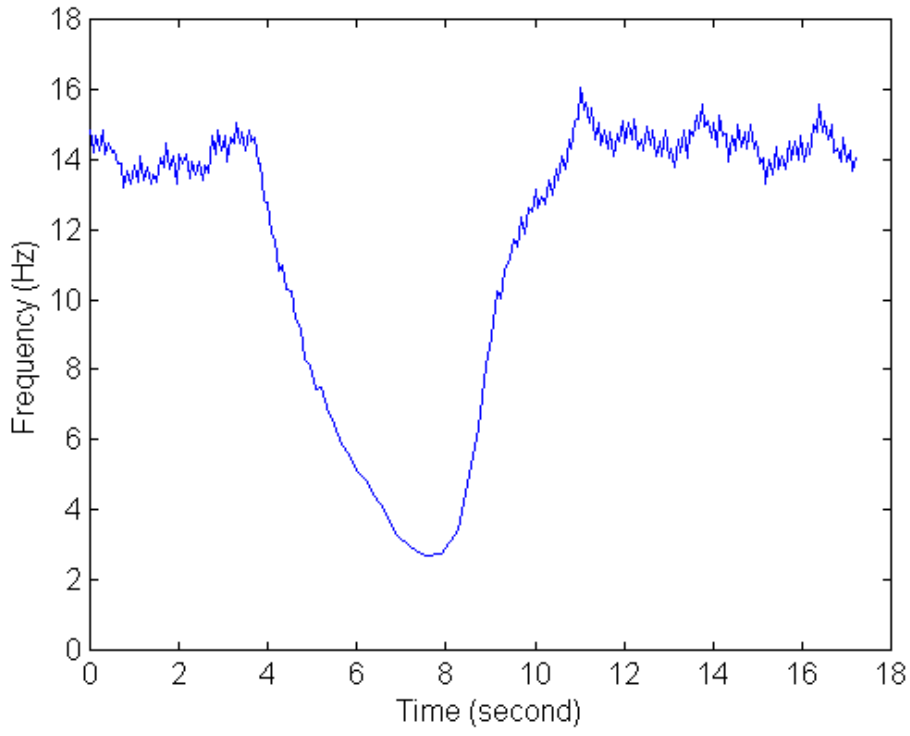

Fig. 1. Curves of the ascending and descending phases of the cup anemometer speed. The wind speed was fixed to 2.84 m s^{-1} (Anemometer 25-2).

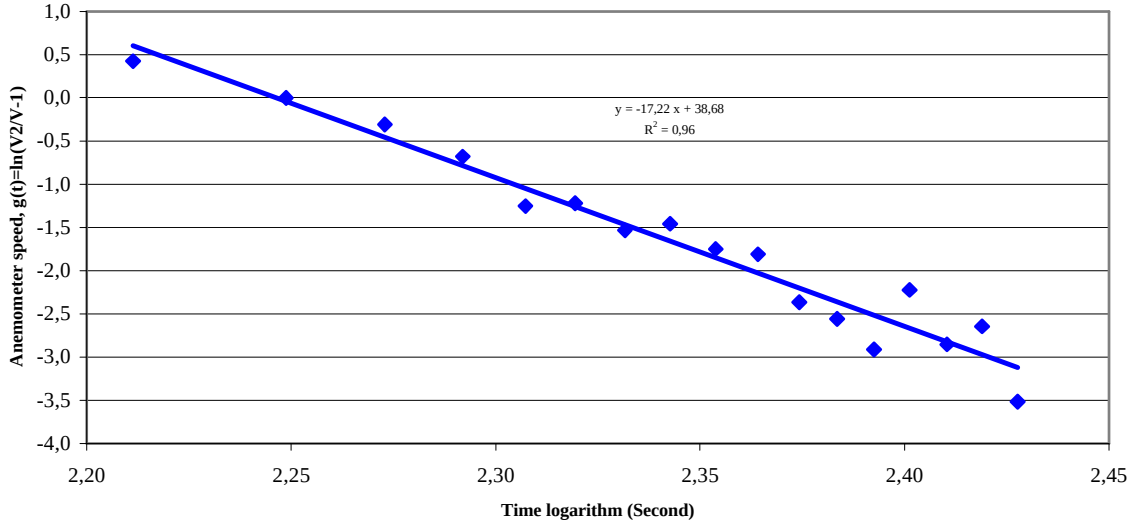

Fig. 2. Anemometer speed function f(t)=V_2/V-1 versus the time, in logarithmic axes with linear regression (Anemometer 25-2).

i) chart the anemometer velocity (in frequency) versus the time;

ii) fit this curve to an exponential (or with a line in logarithmic axes) and extract the coefficient A (see Fig. 2);

iii) calculate the distance constant L with the second relationship of Eq. (10b).

3 Experiments

The experiment, which is an extension of the Wind Erosion and Losses of Soil Nutrients in Semiarid Spain (WELSONS) experiment (Frangi and Richard, 2000), was carried out in an urban area, on the roof of University Paris 7 (Paris, France). The 3.3-m mast supporting the sensors was located at about 20 to 25 m above the ground (Fig. 3).

Fig. 3. Experimental mast including the sonic and the NKE cup anemometers. Heights 20 to 25 m above ground and 3.3 m above the laboratory's building roof.

The equipment consists of two NKE cup anemometers, a Vector cup anemometer A100L2, and a 3-D ultrasonic anemometer. The data of the first two are acquired with a LabView card (National Instruments Company) and rated according to the sample-and-hold technique, in which the time-lag of each rotational fraction is stored until it is replaced by the next one. So the sampling rate of these anemometers, determined by the wind speed, is about 15 Hz for a wind speed of 4 ms^{-1}. The ultrasonic and the Vector cup anemometers are monitored by two Campbell CR10X data-loggers according to the respective sampling rates of 32 and 8 Hz. The ultrasonic anemometer (Campbell CSAT3) has a path-length, d_s, of 10 cm. It measures the wind speed line-averaged along the sonic path d_s. This operation causes a wavelength distortion which, according to Kaimal (1986), is limited to wavelengths smaller than $\lambda_d = 2\pi d_s$.

The two NKE three-cup anemometers, labeled 25-2 and 25-4, have been calibrated in a wind tunnel in 1996 and 1997. Fitted with an opto-electronic transmission system, their overall diameter is 9 cm, with cups of 3 cm in diameter. As for the Vector three-cup anemometer, these dimensions are, respectively, 15 and 5.5 cm. Its calibration parameters, provided by the manufacturer, are variable according to the device angular velocity and they take into account various nonlinearity effects.

Table 1 presents the different periods of the experiment, from July 2002 to February 2003, the mean wind directions, and the timetable of the used sensors.

A second experiment carried out in May and June 2002 in wind tunnels allowed one to determine the NKE cup anemometers distance constants.

4 Results

The NKE cup anemometers data, sampled according to the sample-and-hold technique, normally do not fit to the discrete Fourier transform, since the rating interval is variable. But the comparison between the spectra obtained by applying a discrete Fourier transform and those computed with the periodogram technique, which is a least-squares best fit of sine and cosine waves to the original signal, showed insignificant differences. The same conclusion was reported by Kristensen and Hansen (2002). Thus, the FFT computation technique is applied throughout this study to save time.

Table 2 shows a good correlation between the data provided by the ultrasonic and the cup anemometer, sometimes with a correlation coefficient as large as 0.8. It just means that the two anemometers are within the bigger structures of the flow.

4.1 Spectral compensation and determination of the range of the cup anemometers meaningful spectra

In Fig. 4, one can split the spectrum of the NKE cup anemometer in three regions. In the first one (Part 1) corresponding to the lower frequencies, the two charts (ultrasonic and cup anemometer) nearly merge. In the second region (Part 2), which exhibits the inertial effects of the cup anemometer, the chart of the cup anemometer deviates from the ultrasonic one and from the well-known $-5/3$ slope. The third part (Part 3), a blend of signal and white noises, ends up becoming parallel to the x-axis, thus confirming its typical characteristics (Yim and Chou, 2001).

By combining Eqs. (3) and (5), we obtain the expression of the compensated spectral power, $P_c(\omega)$, of the cup anemometer data as follow:

$$P_c(\omega) = P_a(\omega)\left[1 + \frac{\omega^2 L^2}{U^2}\right]. \tag{11}$$

The application of this equation does not produce similar effects on the above-mentioned different parts of the row spectrum. While in the inertia affected part, the compensation tends to bring the curve slope to the $-5/3$ value, in the white noises affected part, the slope tends towards zero or positive values (Fig. 4). Thus, in the second part, the compensated cup anemometer spectrum approaches the ultrasonic one and deviates from it in the third part. The limit between the two parts represents the upper frequency limit of the meaningful spectrum, later on noted f_{max}.

The cup anemometer maximum accessible frequency, corresponding to the cutoff frequency at the amplitude attenuation coefficient $\alpha = \sqrt{2}/2$ (Guyot, 1997), can be derived from Eq. (6) as follows:

$$f_{co} = \frac{U}{2\pi L}. \tag{12}$$

The ratio of the upper frequency limit to the cutoff frequency, f_{max}/f_{co}, is a performance gauge of both the apparatus and the signal treatment method. Assuming that the ratio of the

Table 1. Different periods of the experiment with the relating mean wind directions and sensors used.

Dates of experiments		July 2002		December 2002				January 2003							February 2003	
		13	16	18	23	26	30	2	14	15	17	20	21	23	4	5
Cup Anemo-meters	NKE 25-2															
	NKE 25-4															
	Vector															
Sonic anemometer																
Wind direction		327	329	65	123	201	199	230	213	156	176	160	156			

Table 2. Data pertaining to the upper frequency limit, f_{max}, the relating amplitude attenuation and the ratio between the previous frequency and the cup anemometer cutoff frequency, f_{max}/f_{co}. Cup anemometer 25-2, date of 30 December 2002.

Sample Start time	Duration	Correlation between the two anemometers	Mean wind speed	Turbulence intensity	Mean f_{max}	Mean amplitude attenuation	Ratio f_{max}/f_{co}
11:10	15 min	0.54	3.50	.41	5	9%	11
11:35	15 min	0.70	3.86	0.46	3	16%	6
12:00	15 min	0.62	4.23	0.40	4	13%	8
12:25	15 min	0.35	3.34	0.46	1	38%	2
12:50	15 min	0.36	3.55	0.38	2	22%	5
13:15	15 min	0.55	3.41	0.44	2	21%	5
13:45	16 min	0.63	4.03	0.36	6	8%	12
14:10	15 min	0.69	3.66	0.37	4	11%	9
14:35	15 min	0.40	2.94	0.43	1	34%	3
15:00	15 min	0.74	3.11	0.39	3	13%	8
15:25	15 min	0.78	2.80	0.37	3	12%	9
15:50	15 min	0.73	2.82	0.35	2	17%	6
16:30	15 min	0.82	2.94	0.38	3	12%	8

variable frequency to the cutoff frequency, f/f_{co}, equals the product of the variable wave number by the distance constant, $\kappa \cdot L$, it becomes more convenient to present the compensated spectrum as a function of the dimensionless wave number, $\kappa \cdot L$ (cf. Fig. 5).

Table 2 presents the main compensation parameters for five samples with mean wind speeds ranging from 2.8 to 4.2 m s^{-1}. The study is restricted to this range because over 5 m s^{-1}, the anemometer inertial effects vanish (the time constant decreasing with the wind speed) and below 2 m s^{-1}, the natural wind is rarely continuous. Thus, one notices that the upper frequency limit, f_{max}, varies from 1 to 6 Hz (i.e. 2 to 12 Hz in temporal mode), for an overall spectral slope less than -1.57 (recalling that $-5/3=-1.67$ and that the slope tends to 0 out of the significant spectrum). These are far above the value of 0.3 Hz reported by Woodward and Sheehy (1983). Figure 6 gives the cumulative distribution of f_{max}. As this frequency is always greater than 1 Hz, for the severe experimental conditions (urban area with turbulence intensity above 0.4), we believe that this value is independent of the mean wind speed but is a characteristic of the anemometer. This hypothesis is reinforced by the fact that the servo-control system of the Vector cup anemometer induces a confinement of the spectra up to 1 Hz (Fig. 7). Similar effects have been observed when the NKE cup anemometer data are uniformly sampled at frequencies close to 10 Hz (through averaging and interpolating operations).

It is generally supposed that higher wind speeds (e.g. over 5 m s^{-1}) lead to wider high frequency spectra (thus, conserving roughly the same wave number, $\kappa = 2\pi f/V$, or scale). However, these results show that this assumption is wrong since the correlation between the upper frequency limit and the mean wind speed vanishes as the latter approaches a certain value (5 m s^{-1}, in this study, cf. Table 3). In this case, reasoning in terms of wave-number parameters only is misleading.

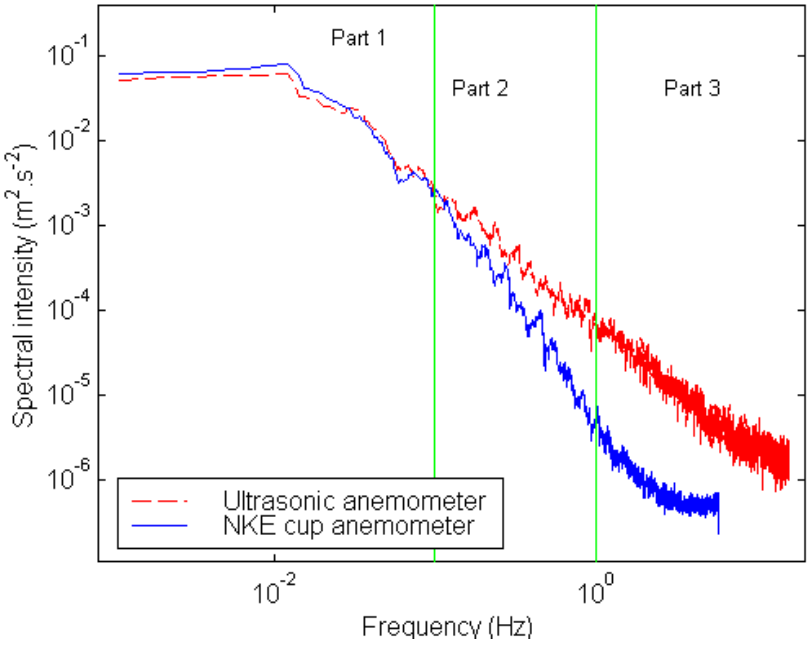

Fig. 4. Spectral intensities of the data from the ultrasonic and the cup anemometers. Sample 4 of 30 December 2002.

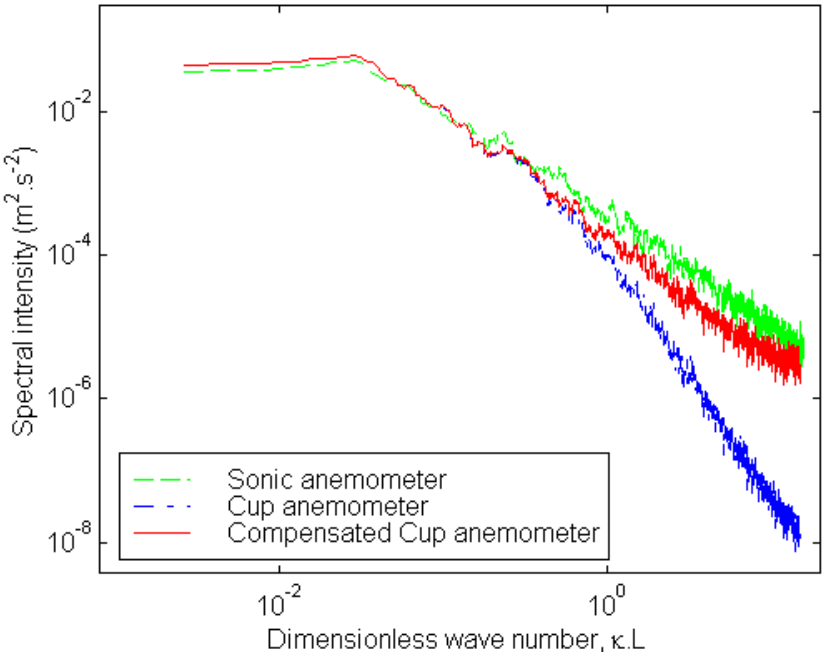

Fig. 5. Spectral intensities of the data from the ultrasonic and the cup anemometers. The third curve represents the compensated data of the cup anemometer. Sample 7 of 30 December 2002.

Beyond 1 Hz, the upper frequency limit of the NKE cup anemometers depends on the wind parameters, particularly the variability of the wind direction, the variation coefficient of the anemometer rotation rate (which is directly linked to the wind longitudinal turbulence intensity) and the mean wind speed (when it is too low, i.e. less than 2.5 m s^{-1}). The standard deviation of the wind direction and the variation coefficient of the anemometer rotation rate are negatively highly correlated to the upper frequency limit (cf. Table 3). This result reveals one of the effects of the two parameters on the cup anemometer behavior. As in the sample-and-hold technique, the sampling rate is determined by the wind speed. At lower speeds the spectral frequency is limited by the rotation rate of the anemometer, thus decreasing

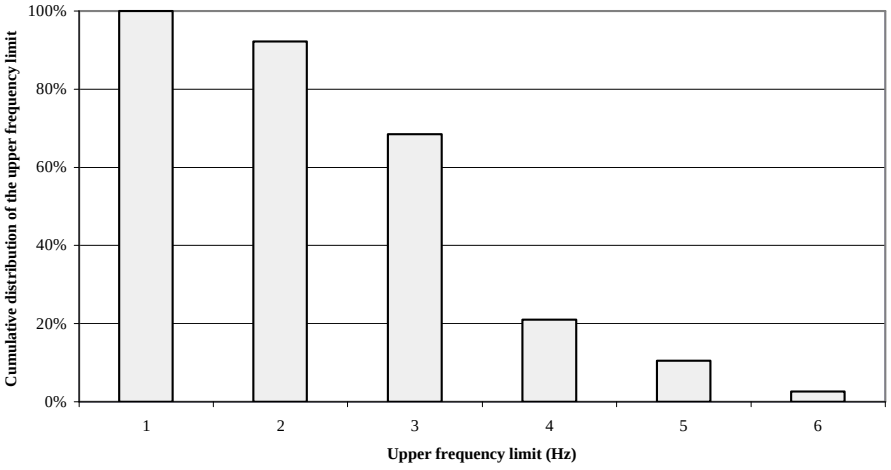

Fig. 6. Cumulative distribution of the NKE 25-2's upper frequency limit.

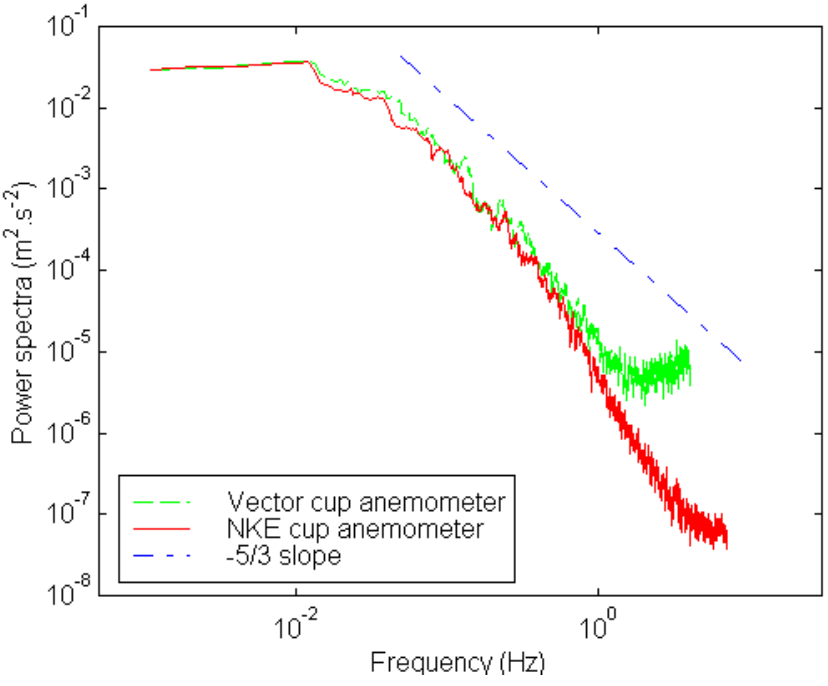

Fig. 7. Comparison between the Vector and the NKE 25-2 cup anemometers spectra (4 February 2003, sample 6).

the upper frequency limit. This explains the positive correlation between the two parameters (cf. Table 3). However, this correlation vanishes when the wind speed increases.

Table 2 also reports the amplitude attenuation rate at the relating upper frequency limit (cf. Eq. 6) and the ratio between this frequency and the cup anemometer cutoff one. We notice that the amplitude attenuation rate at the upper frequency limit can drop down to 12% while the frequency ratio can reach 9. Similar attenuation rates have been reported by Finkelstein et al. (1986) for comparable cup anemometers (distance constant=5 m) at around 0.2 Hz. It appears that, in some cases, one frequency decade can be roughly recovered through the compensation operation. This considerably extends the capacity of cup anemometers which compete with the ultrasonic ones. In many cases, the compensated cup anemometer and the ultrasonic spectra, after correction of the distortion caused by the device length-path, nearly cover the same frequency range (Fig. 5).

4.2 Determination of the distance constant through spectral analysis and comparison with the wind tunnel method

The proposed distance constant determination method relies on the compensation of the power spectrum through the first order transfer function of the anemometer. This supposes that the spectral difference between the cup and the ultrasonic

Table 3. Correlation between, on the one hand, the upper frequency limit and, on the other hand, the mean wind speed, the standard deviation of the wind direction and the coefficient of variation of the cup anemometer rotation rate.

Cup anemometer and dates		NKE 25-2		NKE 25-4	
		26 Dec. 2002	30 Dec. 2002	13 & 16 July 2002	14 & 15 Jan. 2003
Number of studied samples		9	13	12	13
Wind speed variation range ($m\,s^{-1}$)		2.66 to 3.66	2.8 to 3.40	3.52 to 4.07	1.60 to 2.57
Correlation between the upper frequency limit and:	the mean wind speed	0.50	0.56	0.11	0.59
	the Coefficient of variation of the anemometer rotation rate	−0.49	−0.61	−0.31	−0.42
	the standard deviation of the wind direction	−0.41	−0.11	−0.32	−0.25

Table 4. Distance constant values determined through the spectral study (NKE 25-2: dates of 18, 23, 26 and 30 December 2002; NKE 25-4: dates of 13 and 16 July 2002, and 14 and 15 January 2003) and in the wind tunnel.

Anemometer's references	Methodology	Number of studied samples	Distance constant parameters		
			Mean value (m)	Standard deviation (m)	Coefficient of variation
NKE 25-2	Spectral study	38	1.25	0.29	23%
	Wind tunnel study	8	1.22	0.41	33%
NKE 25-4	Spectral study	25	1.23	0.33	27%
	Wind tunnel study	10	1.56	0.45	29%

anemometers data is minimum when the cup anemometer spectrum is corrected through the right distance constant value (see Eq. 5). Table 4 presents the values of two cup anemometers determined through the spectral study.

However, the accuracy of the method depends on the upper frequency limit, since the spectral comparison must be established within the same frequency range. As the deviation of the cup anemometer spectrum increases with the frequency, the greater the upper frequency range, the more accurate the method. Thus, we noticed that the variation coefficient of the determined distance constant decreased from 45 to 25% as the upper limit of the comparison spectral range shifted from 0.5 to 1 Hz (i.e. from 1 to 2 Hz in temporal mode).

Equation (10b) shows that the cup anemometer distance constant can be determined in a wind tunnel by studying the variation of the anemometer angular speed between two given wind speeds, U_1 and U_2. Thus, the distance constants of a set of five NKE cup anemometers (among which NKE 25-2 and 25-4) have been determined in the wind tunnel, for wind speed ranging from 1 to $3\,m\,s^{-1}$ (cf. Table 4). We notice that the values of the distance constant determined in wind tunnel agree well with those stemming from the spectral studies.

4.3 Measurement of the wind variance by cup anemometers

Wind speed variance, which represents the turbulent kinetic energy of the atmospheric flow, is one of the most important parameters conditioning many physical processes in the atmospheric surface layer. Thus, it is involved in the modeling of many atmospheric phenomena, such as the transport and dispersion of air pollutants or the probabilistic wind extreme force.

Although cup anemometers are usually devoted to the measurement of mean wind profiles (Frenzen and Vogel, 2001), some models, however, perform well in the assessment of the wind speed variance within the spectral range of a few Hz (Tangler et al., 1991). Figure 8 compares the wind speed variances measured with the ultrasonic and the NKE cup anemometer, for a sampling rate of 2 Hz (a linear spectral compensation has been applied to the cup anemometer data). Some parameters of the comparison are reported in Table 5. We notice that the slope of the linear regression is very close to 1. However, it remains an offset which could be partly attributed to a calibration discrepancy. We also remark that the regression parameters have been improved by the spectral compensation, making the regression parameters in 2 Hz as good as in 1 Hz. By comparing the relative discrepancy between the two anemometers in 2 Hz, an improvement

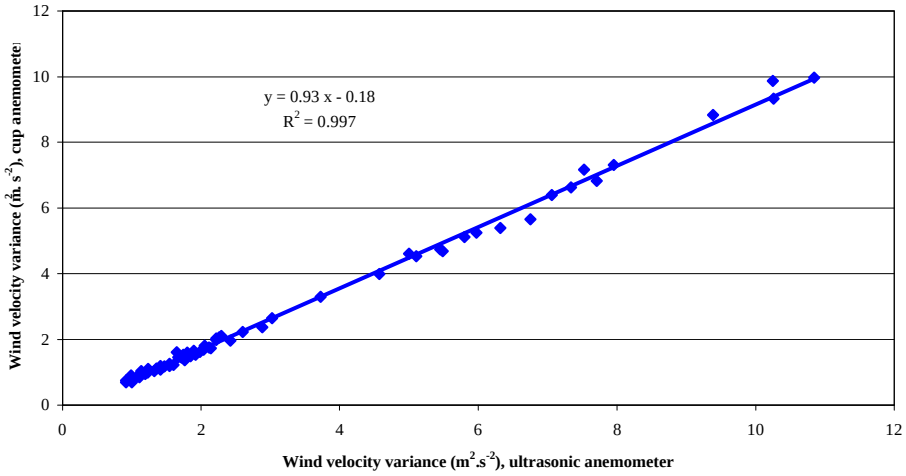

Fig. 8. Comparison of the wind speed variances measured by the ultrasonic and a cup anemometer (NKE 25-2). Sampling frequency of 2 Hz, with spectral linear compensation.

Table 5. Comparison between the wind speed variances from the ultrasonic and the cup anemometer (NKE 25-2). Parameters of linear regression and data relating to the relative underestimation from the cup anemometer.

Sampling rates	1 Hz without compensation	2 Hz without compensation	2 Hz with compensation
Slope a	0.952	0.919	0.932
Linear intercept b	−0.191	−0.201	−0.177
Coefficient of determination (linear correlation) R^2	0.997	0.997	0.997
Mean relative discrepancy between the sets of variances	14 %	18 %	15 %

of about 15% rises. The real rate is expected to be greater than this figure when the possible calibration discrepancy is corrected.

Figure 9 presents the variation, with the mean wind speed, of the relative difference between the wind variances measured by the ultrasonic and a cup anemometer (NKE 25-2). It also shows the effects of the spectral compensation on the data accuracy. To better show the variation of the relative difference, the parameter has been fitted by the function $y=\beta x^{\alpha}$ with which a good correlation (0.7) was found. It appears that, for wind speed above a given threshold (e.g., $5\,\mathrm{m\,s^{-1}}$) and for a spectral range of a few Hz, fast cup anemometers can measure the wind speed variance with errors of the same magnitude as those deriving from the measurement of the mean wind. The latter errors are reported to be within the interval 5–10% (cf. Gouveia and Baskett, 1997).

5 Conclusion

We have presented a method to determine the cup anemometer distance constant from the spectral study of the anemometer response to the natural wind turbulence. Even if the study relied on the use of an ultrasonic anemometer as a reference, its presence was not necessary since one could rely on the $-5/3$ spectral slope of the turbulence inertial sub-range. However, two main conditions are required for accurate data: low mean wind speed that can generate significant inertial effects on the anemometer response and a prior determination of the device upper frequency limit. The lowest value of the upper frequency limit can be defined as a characteristic of the cup anemometer. Its knowledge could also constitute a guideline in the choice of an experimental sampling rate.

This study also showed how far it was possible to go in the compensation of the cup anemometer data. It offers a prospect in the improvement of the device'sd own capacities. A practical conclusion is that the wind speed variance could be measured, with acceptable errors, by fast cup anemometers within a spectral range of few Hz for wind speed exceeding $5\,\mathrm{m\,s^{-1}}$. The spectral compensation, which presents an improvement of the measurement accuracy by some 15%, could help to improve the data measurement, particularly for the lower speeds.

However, further studies are necessary, on the one hand, to confirm the values of the upper frequency limit in a less

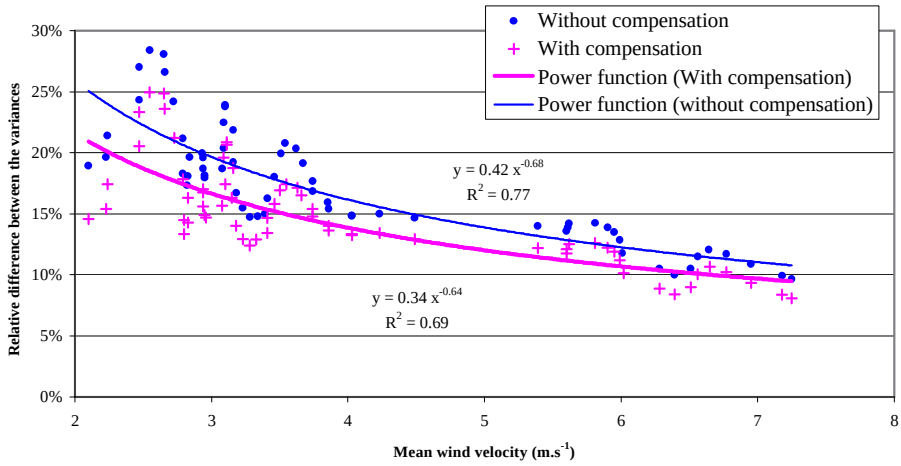

Fig. 9. Relative difference between the wind variances measured by the ultrasonic and a cup anemometer (NKE 25-2). Variation with the mean wind speed and effects of the spectral compensation (Sampling frequency of 2 Hz).

turbulent environment (low turbulence intensity) and, on the other hand, to explain the observed offset (beyond the improvement achieved through the spectral compensation) between the variances provided by the two anemometers models. In the latter case, investigations could focus on better calibration methodology, taking into account the anemometer rotation range.

Appendix A

From Eq. (2), we have:

$$\tau \frac{ds'(t)}{dt} + s'(t) = \frac{1}{l}\left(u'(t) + \mu w'(t)\right) . \tag{A1}$$

If F(ν) is the Fourier transform of the time function $f(t)$, then we have:

$$\frac{df(t)}{dt} \Leftrightarrow (2\pi j\nu)\, F(\nu) , \tag{A2}$$

where j is the complex number for which $j^2{=}{-}1$.

With T_x the Fourier transform of the function $x'(t)$, the Fourier transform of Eq. (A1) is:

$$T_s(\nu)\,(2\pi j\nu\tau + 1) = \frac{1}{l}\left(T_u(\nu) + \mu T_w(\nu)\right) . \tag{A3}$$

In terms of spectral powers, the equation becomes:

$$P_s(\omega)\,|\omega\tau j + 1|^2 = \frac{1}{l^2}\left(P_u(\omega) + \mu^2 P_w(\omega) + \mu P_{uw}(\omega)\right) \tag{A4}$$

with P_{uw} the cross-spectrum of u' and w'. The transfer function, $F_T(\omega)$, of the anemometer is as follows:

$$F_T(\omega) = \frac{l^2 P_s(\omega)}{P_u(\omega) + \mu^2 P_w(\omega) + \mu P_{uw}(\omega)} \approx \frac{1}{1+\omega^2\tau^2} . \tag{A5}$$

Replacing the time constant, τ, by its expression of Eq. (4), Eq. (A5) transforms into:

$$F_T(\omega) = \frac{1}{1 + \frac{\omega^2 L^2}{U^2}} . \tag{A6}$$

Appendix B

The characteristic equation of the anemometer response to low wind variation around a speed U is reported by Kristensen and Hansen (2002) as:

$$\tau \frac{ds(t)}{dt} + s(t) = \frac{1}{l}\left(u(t) - U_0\right) . \tag{B1}$$

In laminar flow, for a wind speed variation between U_1 and U_2, the previous equation becomes:

$$\tau \frac{ds(t)}{dt} + s(t) = \frac{1}{l}\left(U_2 - U_0\right) . \tag{B2}$$

One should remember that the value U_1 does not intervene in this step, where the forcing parameter is the difference $U_2{-}(U_0{+}ls(t))$. Thus, the Eq. (B2) becomes:

$$\frac{ds(t)}{dt} = \frac{1}{\tau l}\left(U_2 - ls(t) - U_0\right) . \tag{B3}$$

From Eq. (4), one can write:

$$\tau = \frac{L}{U} = \frac{L}{ls(t) + U_0} . \tag{B4}$$

Combining with this equation, Eq. (B3) becomes:

$$\frac{ds(t)}{dt} = \frac{ls(t) + U_0}{lL}\left(U_2 - ls(t) - U_0\right) . \tag{B5}$$

And from this:

$$\frac{ds(t)}{\left(ls(t) + U_0\right)\left(U_2 - ls(t) - U_0\right)} = \frac{U_2}{lL}dt \tag{B6}$$

or

$$\frac{ds(t)}{ls(t)+U_0}+\frac{ds(t)}{U_2-ls(t)-U_0}=\frac{U_2}{lL}dt\,. \tag{B7}$$

Integrating the previous equation, one obtains:

$$\ln\left(\frac{lS+U_0}{U_2-U_0-lS}\right)$$

$$-\ln\left(\frac{lS_1+U_0}{U_2-U_0-lS_1}\right)=\frac{U_2}{L}\,(t-t_1)\,. \tag{B8}$$

Abbreviations and acronyms

ASL	Atmospheric Surface Layer
FFT	Fast Fourier Transform
LED	Laboratory Environment and Development
NKE	Cup anemometer manufacturer
WELSONS	Wind Erosion and Losses of Soil Nutrients in semiarid Spain experiment

List of symbols

d_s	sonic anemometer path length
f	frequency
f_{co}	cutoff frequency
f_{max}	upper frequency limit of the meaningful spectrum
F_T	cup anemometer transfer function
j	complex number
l	Calibration constant
L	distance constant
P_a	spectral intensity of the cup anemometer speed
P_c	Compensated spectral intensity of the cup anemometer response
P_s	spectral intensity of the cup anemometer angular velocity
P_u	spectral intensity of the longitudinal wind speed
P_{uw}	cross spectral intensity of the longitudinal and the vertical wind speeds
P_w	spectral intensity of the vertical wind speed
s	cup anemometer angular velocity
S	mean angular velocity of the cup anemometer
s'	fluctuations of the cup anemometer angular velocity
S_i	mean angular velocity of the cup anemometer at time i
t	the time
t_1	initial time
u	wind speed
u'	fluctuation of the longitudinal wind speed
u_a	wind speed furnished by cup anemometer
U	mean wind speed
U_0	threshold wind speed
U_i	mean wind speed at time I
V	mean wind speed
w'	fluctuation of the vertical wind speed
α	amplitude attenuation coefficient
κ	wave number
λ_d	wave length of wind speed fluctuations
μ	constant
τ	cup anemometer time constant
ω	pulsation

Acknowledgements. The authors would like to thank N. Crescenzo, Director France, Campbell Scientific Ltd., for the lending of some measurement instruments.

Topical Editor O. Boucher thanks two referees for their help in evaluating this paper.

References

Finkelstein, P. L., Kaimal, J. C., Gaynor, J. E., Graves, M. E., and Lockhart, T. J.: Comparison of wind monitoring systems, Part I: in situ sensors, J. Atmos. Oceanic Technol., 3, 583–593, 1986.

Frangi, J. P. and Richard, D. C.: The WELSONS experiment: overview and presentation of first results on the surface atmospheric boundary-layer in semiarid Spain, Ann. Geophys., 18, 365–384, 2000.

Frenzen, P.: Fast response cup anemometers for atmospheric turbulence research, Proc. Eight Symp. on Turbulence and Diffusion, San Diego, CA, Amer. Meteor. Soc., 112–115, 1988.

Frenzen P. and Vogel C. A.: Further studies of atmospheric turbulence in layers near the surface: scaling the budget above the roughness sub-layer. Bound.-Layer Meteorol., 99, 173–206, 2001.

Gouveia F. J. and Baskett R. L.: Evaluation of a new sonic anemometer for routine monitoring and emergency response application, Sixth Topical Meeting on Emergency Preparedness and Response, San Francisco, CA, April 22–25, 1997.

Guyot G.: Climatologie de l'environnement – De la plante aux écosystèmes, edited by: Masson, Coll. SV, Paris, 505, 1997.

Hristov, T. S., Miller, S. D., and Friehe, C. A.: Linear Time-Invariant Compensation of Cup Anemometer and Vane Inertia, Bound.-Layer Meteor. 97, 293–307, 2000.

Kaimal, J. C.: Flux and profile measurements from towers in the boundary layer, in: Probing the Atmospheric Boundary Layer, edited by: Lenschow, D. H., Amer. Meteorol. Soc., 19–28, 1986.

Kristensen, L.: Cup Anemometer Behavior in Turbulent Environments, J. Atmos. Oceanic Tech., 15, 5–17, 1998.

Kristensen, L. and Hansen, O. F.: Distance Constant of the Risø Cup Anemometer, Technical Report Risø-R-1320 (EN), Risø National Laboratory, Roskilde, Denmark, 2002.

MacCready, P. B. and Jex, H. R.: Response characteristics and meteorological utilisation of propeller and vane wind sensors, J. Appl. Meteorol., 4, 182–193, 1964.

Makkonen L., Lehtonen P., and Helle, L.: Anemometry in icing conditions. J. Atmos. Oceanic Tech., 18, 1457–1469, 2001

Tangler, J., Smith, B., Kelley, N., and Jager, D.: Measured and predicted rotor performance for the SERI advanced wind turbine blades, Proc. Windpower '91, American Wind Energy Association, 199, 104–110, 1991.

Weber, R. O.: Estimators for the standard deviations of the lateral, longitudinal and vertical wind components, Atmos. Environ., Vol. 32, No. 21, 3639–3646, 1998.

Woodward, F. I. and Sheehy, J. E.: Principles and measurements in environmental biology,l Butterworths, London, 1983.

Yahaya, S.: Dynamique de la couche limite de surface semi-aride: Approche des caractéristiques turbulentes par anémométrie à coupelles et effet des traitements de surface du sol, Thèse de doctorat de l'Université Paris 7 Dénis Diderot, 248, 2004.

Yahaya, S., Frangi, J. P., and Richard, D. C.: Turbulent characteristics of a semiarid Atmospheric Surface Layer from cup anemometers – Effects of soil tillage treatment (Northern Spain), Ann. Geophys., 21, 2119–2131, 2003.

Yim, J. Z. and Chou, C.-R.: A study of the characteristic structures of the strong wind, Atmos. Res. 57, 151-170, 2001.